



Research



PV based OFF grid charging station for E-vehicles using PWM and phase shift controlled interleaved three port converter

Kudiyarasan Swamynathan¹ · N. Mahalingam¹ · Alagumariyappan Paramasivam² · Sankaran Vijayalakshmi³

Received: 12 April 2023 / Accepted: 2 November 2023

Published online: 14 November 2023

© The Author(s) 2023 **OPEN**

Abstract

In recent years, Electric Vehicles are becoming more popular. The pollution level in the atmosphere can be effectively minimized by using Electric vehicles for large-scale transportation. A battery station is required for continuous operation; however, the Photovoltaic-based OFF grid charging station can only operate during the day. Therefore, the three-port converters have started to arise from a number of current EV charging station developments. In this study, a unique PWM and Phase Shift Controller are proposed to reduce switching losses and to improve reliability. In addition, for Maximum PowerPoint Tracking, a Fuzzy is added to the PV system. Furthermore, an appropriate interleaved boost converter topology is used to create the various charging voltages required for EV and battery stations. The proposed topology is simulated, and the hardware prototype has been created and tested. The result shows that the proposed topology has a better efficiency than the traditional converters.

Article Highlights.

- A dual composite charging station for electric vehicle charging in environment friendly manner.
- Optimization of power electronics required in Electric Vehicle charging stations.
- Maximum utilization of battery for cyclic charging from charger and discharging through Electric Vehicles.

Keywords Charging station · Electric vehicle · OFF-GRID · Photovoltaic · PWM converter

Abbreviations

BDBC	Bi-directional boost converter	MPPT	Maximum power point track
CC	Constant current	PIC	Programmable interface controllers
ESS	Energy storage station	PV	Photo voltaic
EV	Electric vehicle	PWM	Pulse width modulation
EVCS	E-vehicle charging station	TPC	Three port converter
FLC	Fuzzy logic controller		

✉ Kudiyarasan Swamynathan, kudiyarasan@rediffmail.com; N. Mahalingam, mahalingam@bhavini.in; Alagumariyappan Paramasivam, draparamasivam@veltech.edu.in; Sankaran Vijayalakshmi, drvijayalakshmis@veltech.edu.in | ¹Electrical Group, DAE, Bharatiya Nabhikiya Vidyut Nigam Limited, Kalpakkam, Tamilnadu 603102, India. ²Department of Electronics and Communication Engineering, Vel Tech Rangarajan Dr. Sagunthala R&D Institute of Science and Technology, Chennai, India. ³Department of Bio Medical Engineering, Vel Tech Rangarajan Dr. Sagunthala R&D Institute of Science and Technology, Chennai, India.



SN Applied Sciences

(2023) 5:331

| <https://doi.org/10.1007/s42452-023-05571-w>

1 Introduction

In recent years, renewable energy sources such as solar and wind have gained more significance. Furthermore, the most prevalent method of generating electrical energy which utilizes solar sources has resulted in the creation of numerous converter topologies [1]. For higher-power applications, the integrated multiport converter is preferred [2]. The Electric Vehicle (EV) requires a wide range of voltage and current ratings, which have resulted in the creation of a wide range of, boost converter topologies with minimal losses [1]. The development of OFF-grid three port converters (TPC), which are widely employed in the automobile sector in any developing country [3] leads to the generation of electricity at remote locations, storage, and charging of EV vehicles.

The photovoltaic power generating station (PPGS), DC-DC Bi-directional boost converter (BDBC), Energy storage station (ESS), and E-Vehicle charging station (EVCS) are all displayed in the TPC [4]. In terms of voltage and current, the PV array converts solar energy into clean electrical energy. The resulting voltage is fed into the boost converter, which eliminates irradiance variations [4].

As a result, a Maximum Power Point Track (MPPT) approach is used. The MPPT harvests the greatest power from the PV array and provides the boost converter with the appropriate operating voltage and current. Furthermore, the boost converter generates Pulse Width Modulation (PWM) signals from the MPPT to produce the output voltage according to the desired DC-link voltage. The EVCS and ESS are connected to the DC-link voltage at the DC bus. Other literature surveys were investigated and presented here.

The nine distinct traditional types of TPC were investigated, and it was simulated with two different switching frequencies total switching and conduction classes when available, as well as the efficiency of each scenario [1]. This research presented a comparative study and the numerous benefits of different types of solar charging Stations, including how they solar PV output conventional load and the electric car models are realised, as well as a comparison of their efficiency with respect to varying irradiation [5]. A multiport converter is used in an E vehicle that is drawn by a switch electric motor and the potential energy of the vehicle is used during braking to charge a battery generator control unit is also coupled for high speed running during acceleration to climb height generator control unit and battery unit working both together the DC-DC converter taking all synchronization whenever required [2]. This is accomplished by the use of a directed DC-DC converter connected to

the grid with a synchronized static compensator and an active power filter, which considerably reduces reactive power [6]. The double boost input output converter is used in this TPC for better impedance matching and stable DC bus, which in turn properly maintains the maximum power and the DC bus voltage variation, is compensated in the second stage boost converter [7].

By connecting a parallel resonance circuit in series with the battery, very fast charging is enabled. The tank impedance (LC) and battery source impedance are set to saturate the boost charging current limit crossings, resulting in excess initial charging [8]. TPC duty cycle should be charged dynamically to adjust for the last and effective power implication. Many modes are addressed in this study, and the duty cycle of various parts is estimated using volt second balance integrated, and the duty cycle correlation is determined for various dynamic scenarios. [9]. In a traditional report converter, there will be a mass of DC-DC converter that will match the impedance between the PV panel and the battery and the PV panel and the load. In this paper, TPC is used with soft switching techniques that will take care of MPPT under the Impedance matching between the battery and the load [10]. DC bus with a high voltage there are two steps of power conversion that are performed: the first stage is for MPPT, and the second stage is to synchronize all the outputs to build the high voltage DC bus. Series connection of DC-DC converters and choppers is achieved. Instead of using high voltage switching, this topology can be thought of as soft switching [11]. To upgrade the electric car when a group connected system is used, the modified switching algorithm is used. When the DC bus voltage shoots up, the excess voltage is dropped down by switching on to MOSFETs. When the DC bus is stable, one switch breaks, and stable DC voltage is applied to EV [12].

A closed loop current controller is a type of current controller. The PI regulator and hysteresis PWM controller switch the DC-DC converter to decrease the lead or lagging angle between voltage and current so that the source power is effectively used for EV [13]. MPPT DC to DC Converter and grid synchronized inverters are connected with a common DC link and an isolated charger is connected to the DC link to charge the EV. The output impedance of the PV panel is matched with the DC link by MPPT depending on the high power [14]. Large PV panels are coupled in series and parallel configurations during HDC transmission in order to inhibit the ability to function in discontinuous current mode for zero current switching, which in turn speeds up semiconductor device switching considerably. The identical arrangement of medium voltage PV panels is used in this paper, and simulation was used to confirm it [15].

BDBC have grown in popularity in recent years. It is a bidirectional three-port DC-DC converter with fewer switches that can accept multiple inputs such as a PV array and a battery end. Soft switching is achieved through the use of LCL resonance circuitry and isolation. The energy held in the ESS is returned to the DC-link via the BDBC, which is in boost mode. The Constant Current (CC) control approach is used to carry out the conversion mode [16]. The control technique uses microcontroller-based PWM to create PWM signals [17]. The control signal generated by the control strategy adjusts the converter's mode of operation (boost or buck) [18].

In general, the ESS has a battery bank which is used as an energy saver during periods of high energy generation and is fully utilized [5, 19]. The boost converter allows the ESS to use solar energy. Solar energy charges the e-vehicle in normal conditions, and if solar power is unavailable, the battery feeds the EVCS via the BDBC and semi-bridge converter. EVCS use the BDBC, isolation transformer, and semi-bridge converter to get electricity from solar or ESS [20].

Overall, an integrated TPC offers excellent dynamic performance as well as high efficiency [21]. Also, it is essential to have an optimum utilization of battery for cyclic charging and discharging operations. In this way, the proposed work is a dual composite charging station for electric vehicle charging which utilizes less power electronics component count. The proposed three port converter is specially designed for EV charging application which consists of three different ports out of which two ports are utilized as an output ports. One port can be utilized to charge a battery and other can be utilized for EV charging. Also, the advantages of Fuzzy based MPPT techniques such as excellent handling of non-linearity and uncertainty in PV applications were observed through literatures. So, it is adopted for the present work. The objective of this work is to propose a Photo Voltaic (PV) based OFF-grid charging station for electric vehicles that uses PWM and a Phase Shift Controlled Interleaved Three Port Converter. Also, the proposed system is equipped with fuzzy based MPPT since the system is connected to PV system. Also, the proposed novel method provides a maximum utilization of battery for both charging and discharging operations.

The schematics and the mode of operation and the MPPT technique adopted for the proposed three port converter is explained in the Sect. 2 to Sect. 6. Further, the PWM generation and the sequence of switching operation are discussed in Sect. 7 and 8 respectively. Also, the simulation and the experimental results of the proposed system are disclosed and explained in the Sect. 9 and 10. The observations are also concluded in Sect. 10.

2 Schematic of three port converter

The schematic of a three-port converter is shown in Fig. 1. The TPC has three ports: the first one is the input port that receives DC power from the solar energy system, and the second and third are output ports that supply power to the ESS and EVCS.

3 Solar energy feed to ESS and EVCS

Figure 2a and b depicts the Mode-1 operation of solar power feed to ESS and EVCS. In this mode, the solar power is provided to both the ESS and the E-Vehicle Station via a boost converter and a semi-bridge converter.

The positive (+Ve) voltage is extended to ESS through inductor L1 & M1 at time T1, whereas the negative (-Ve) voltage is directly connected to ESS through MOSFET switches M1 & M4. Simultaneously, the isolation transformer receives positive (+Ve) from inductor L1 and negative (-Ve) from M4, before feeding isolation power to EVCS via a semi-bridge converter. The output semi-bridge converter is connected at the isolator. The diodes D1 and M6 conduct during the positive half cycle, and the output voltage appears across the EVCS. At time T2, the MOSFET switches M2 & M3 conduct, extending the positive (+Ve) voltage to ESS through inductor L2 and M2, while the negative (-Ve) voltage is linked directly to ESS. At the same time, the isolation transformer receives positive (+Ve) from inductor L2 and negative (-Ve) from M3, before feeding power to EVCS via a semi-bridge converter. The diode D2 and MOSFET M5 conduct at the isolation output in the negative half cycle, producing the output voltage across the EVCS. Across the ESS and EVCS, this voltage is filtered and regulated DC appears as an output. The

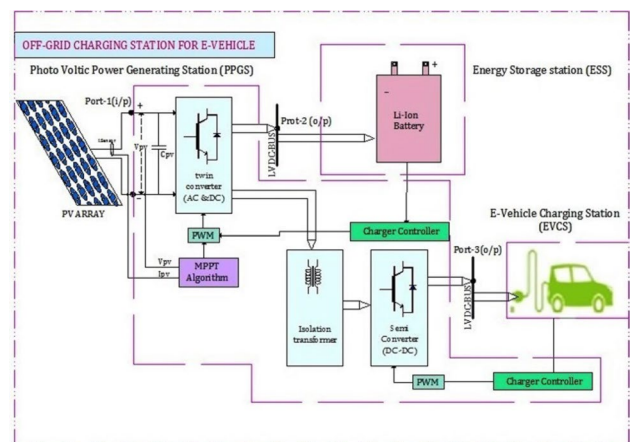
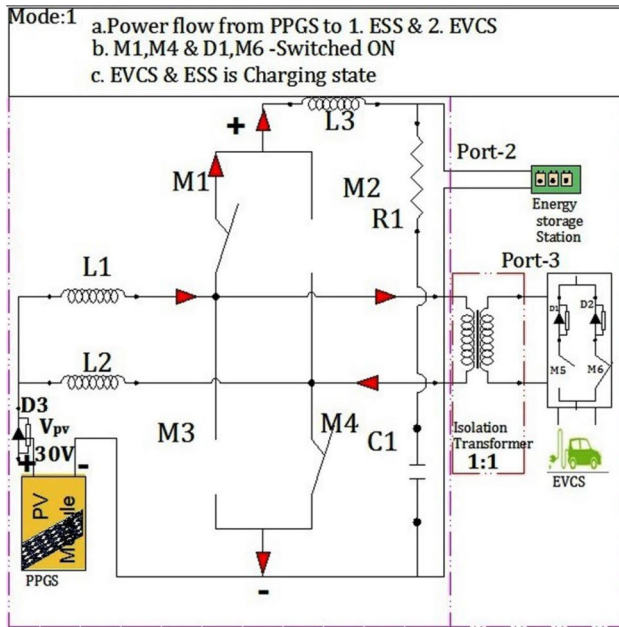
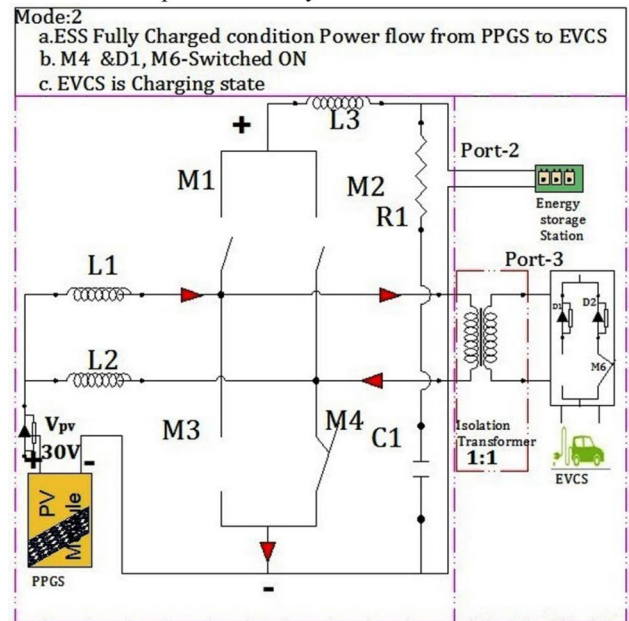


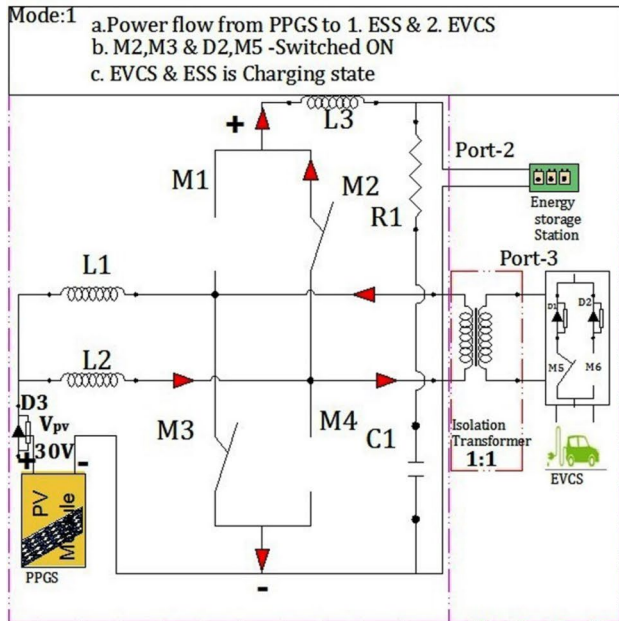
Fig. 1 Schematic of OFF-Grid three port charging station



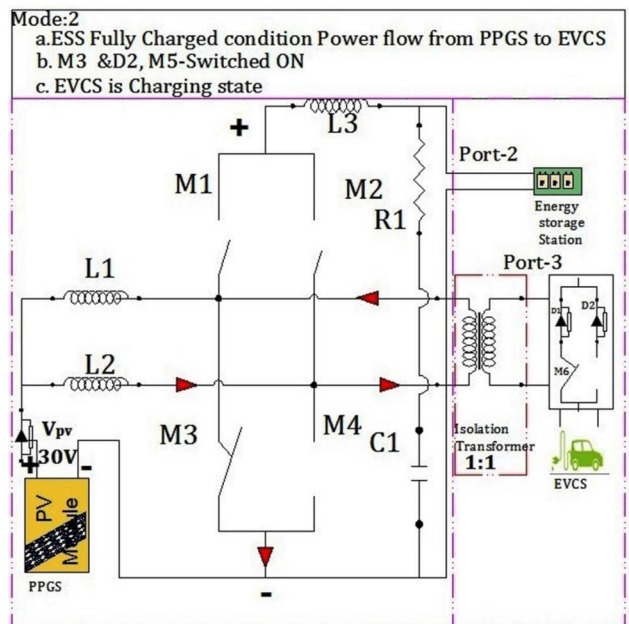
(a)



(a)



(b)



(b)

Fig. 2 **a** Mode-1 operation of solar power feed to ESS and EVCS with M1 and M4 ON condition. **b** Mode-1 operation of solar power feed to ESS and EVCS with M2 and M3 ON condition

Fig. 3 **a** Power flow diagram of mode-2 operation with M4 ON condition. **b** Power flow diagram of mode-2 operation with M3 ON condition

microcontroller-based 6 pulse PWM generator controls the ON and OFF time switching of MOSFET switches.

4 Solar energy feed to EVCS

The typical circuit diagram and mode 2 operation of solar power feed to EVCS via DC-DC converter and semi-bridge converter is shown in the Fig. 3a and b. In this mode, the ESS battery is fully charged, and solar energy is directed solely to the E-Vehicle station via a boost converter and

semi-bridge converter. At time T1, the positive (+Ve) voltage was extended to the isolation transformer via inductor L1, and the negative (−Ve) voltage was received via M4, with the isolation transformer power being fed to the EVCS via a semi-bridge converter. The semi-bridge converter is linked to the isolation output, and the output voltage emerges across the EVCS when the diode D1 and M6 conduct at positive half cycle.

At time T2, the positive (+Ve) voltage extended isolation transformer is fed to EVCS via inductor L2 and the negative (−Ve) voltage is fed to EVCS via M3. The isolation transformer power is then fed to EVCS via a semi-bridge converter. The diode D2 and M5 conduct at the isolation output in the negative half cycle, and the output voltage emerges across the EVCS. This voltage is filtered, and the regulated DC appears across the EVCS.

5 Solar energy feed to ESS

The typical circuit diagram and mode 3 operation of solar power supply to ESS via DC-DC converter and semi-bridge converter is shown in Fig. 4a and b.

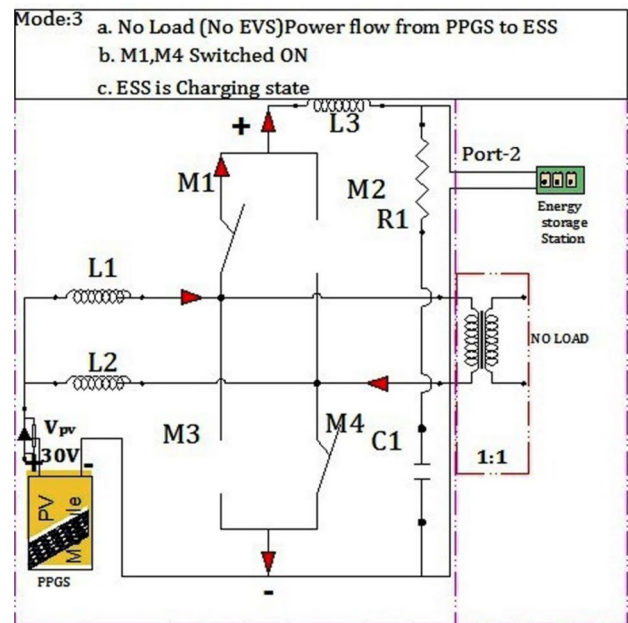
Solar power is directed solely to the Energy Storage Station in this mode, via a boost converter and semi-bridge converter. The MOSFET switches M1 and M4 conduct at time T1, extending the positive (+Ve) voltage to ESS through inductor L1 and M1, while the negative (−Ve) voltage is directly linked to ESS.

At time T2, the MOSFET switches M2 and M3 conduct, extending the positive (+Ve) voltage to ESS through inductor L2 and M2 and directly connecting the negative (−Ve) voltage to ESS. This voltage is filtered which results in pure DC across the ESS.

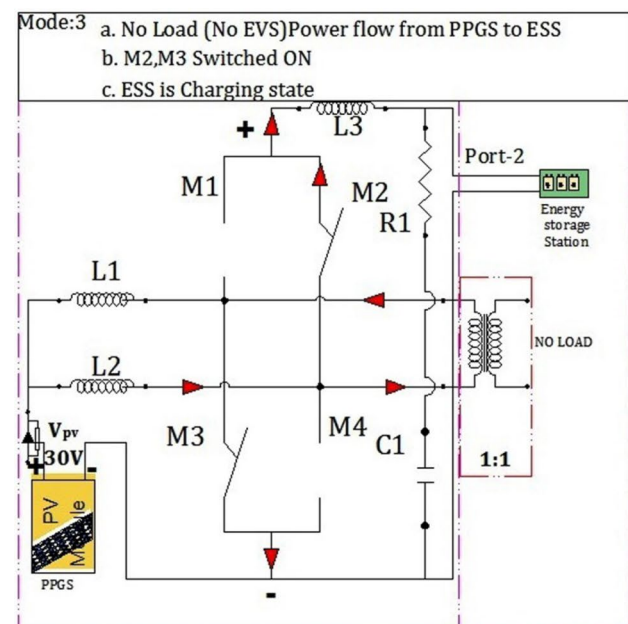
6 ESS energy feed to EVCS

Figure 5a and b depicts a typical circuit diagram and mode 4 operation of the ESS feed to the EVCS through a DC-DC converter and a semi-bridge converter. Solar power is not accessible in this mode, so the diode D3 operates as an open circuit, while the stored energy from the ESS is fed to the E-Vehicle station via a boost converter. The MOSFET switches M1 and M4 conduct at time T1. The isolation power supply to EVCS via a semi-bridge converter at positive half cycle across the isolation transformer. In addition, the diodes D1 and M6 current, resulting in output voltage across the EVCS.

The MOSFET switches M2 and M3 conduct at time T2. The power is fed to EVCS via a semi-bridge converter in the negative half cycle across the isolation transformer. The output voltage emerges across the EVCS after the



(a)



(b)

Fig. 4 **a** Circuit diagram of mode-3 operation with M1 and M4 ON condition. **b** Circuit diagram of mode-3 operation with M2 and M3 ON condition

diode D2 and M5 conduct. Fuzzy logic controller (FLC) is the popular approach for MPPT nowadays. The FLC has four main steps namely Fuzzification, Fuzzy inference, Fuzzy rule base and De-fuzzification. The FLC has the following advantages such as robust appearance, work with imprecise inputs, better handling of non-linearity. It uses fuzzifier for the process of fuzzification. The most

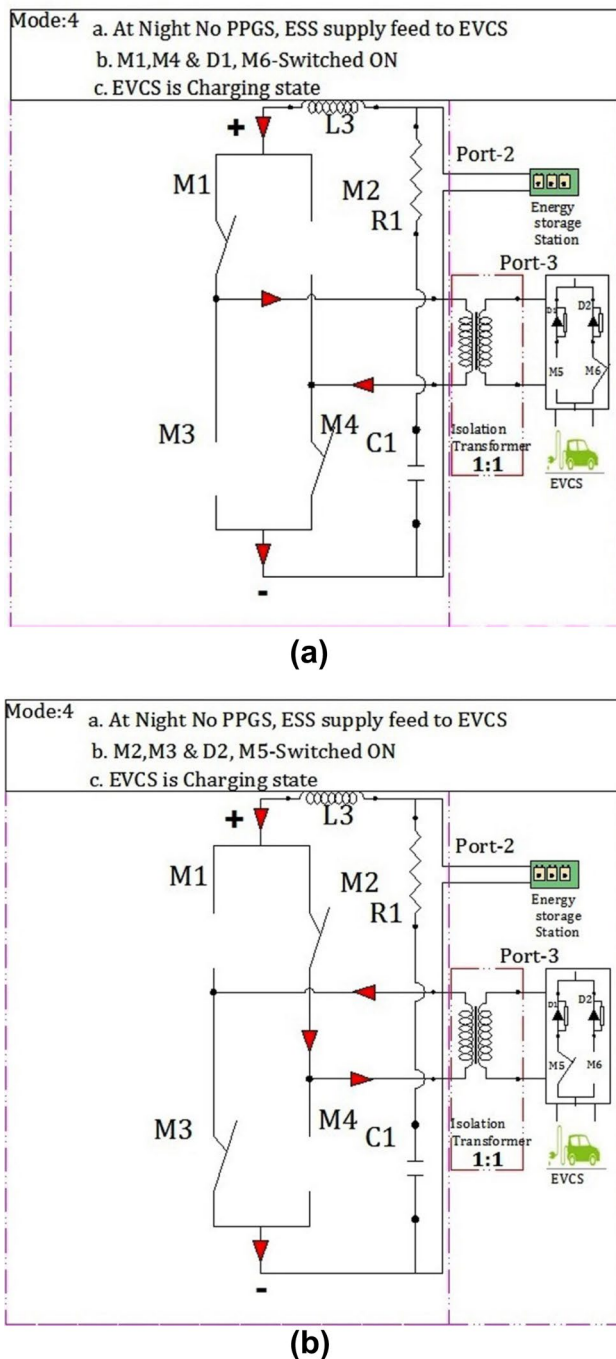


Fig. 5 **a** Power supply feed diagram of mode-4 operation with M1 and M4 ON condition. **b** Power supply feed diagram of mode-4 operation with M2 and M3 ON condition

commonly used type is Mamdani fuzzifier. The input values given to fuzzifier are current (I_{pv}) and voltage (V_{pv}) of PV panels which calculates the power (P_{pv}). The error (E) and change in error (ΔE) from fuzzifier is given

as input to fuzzy inference. The fuzzy inference is performed by fuzzy Rule base (Decision making algorithm). The output of fuzzy inference is given to defuzzifier and these outputs are the changes in duty cycle of MOSFET switches. In addition, Table 1 represents the MPPT Fuzzy rule.

The set of linguistic values (NB, NM, NS, ZE, PS, PM, PB) represents "negative large," "negative medium," "negative small," "zero," "positive small," "positive medium," and "positive big". A fuzzy controller's set of language rules is its most important component. In many circumstances, converting an expert's experience into these rules is simple, and any number of such rules can be developed to specify the controller's behaviors.

The suggested Fuzzy MPPT technique's logical flow diagram is shown in Fig. 6. The maximum power is tracked continually to optimize the system efficiency because the PV panel is employed as an input DC power source. The proposed MPPT's logical flow is shown in the Fig. 6, and the functioning is clearly explained.

The PV panel's output voltage (V_{pv}) is given in Eq. 1, and the PV panel's output power (P_{pv}) is given in Eq. 2. In addition, Eqs. 3 through 6 contain all of the linked equations.

$$\begin{aligned} \text{Output of } V_{pv} &= V_1 = VPV (n - 1) \\ &= V_2 > V_{pv} (n) \end{aligned} \tag{1}$$

$$\begin{aligned} \text{Power Output of } P_{pv} &= P_1 = P_{pv} (n - 1) \\ &= P_2 < P_{pv} (n) \end{aligned} \tag{2}$$

$$P_{pv}(n - 1) < P_{pv}(n) \tag{3}$$

$$P_{pv}(n - 1) > P_{pv}(n) \tag{4}$$

$$P_{pv} = P_{pv}(n - 1) \tag{5}$$

$$V_{pv} = V_{pv}(n - 1) \tag{6}$$

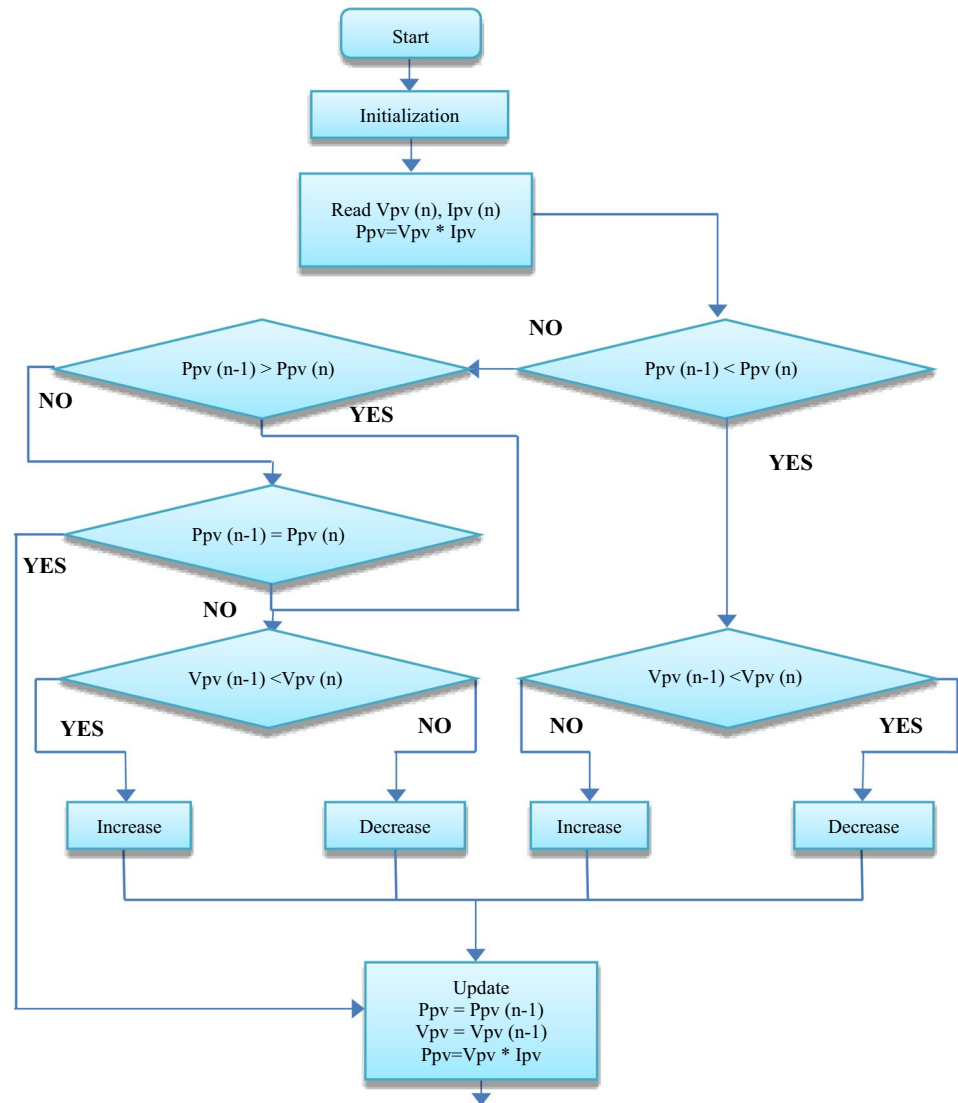
7 PWM controller block diagram

The microcontroller based PWM generator consists of sub-components such as Analog to Digital (AD)/Digital to Analog (DA) cards, comparators, amplifier feedback controllers, crystal oscillator, and pulse generator. Figure 7 shows a general block diagram of a PWM controller.

Table 1 MPPT-fuzzy rule table

$\Delta(e_k)\backslash\Delta(P_k)$	NB	NM	NS	ZE	PS	PM	PB
NB	PB	PB	PM	PM	PS	ZE	ZE
NM	PB	PM	PM	PS	ZE	ZE	NS
NS	PM	PM	PS	ZE	ZE	NS	NS
ZE	PM	PS	ZE	ZE	NS	NS	NM
PS	PS	ZE	ZE	NS	NS	NM	NM
PM	ZE	ZE	NS	NS	NM	NM	NB
PB	ZE	ZE	NS	NS	NM	NM	NB

Fig. 6 Logical flow diagram for proposed MPPT



The microcontroller based PWM generator takes the input signal from PV module and outputs through a MPPT, boost converter outputs and semi bridge converter outputs etc., (i.e., I_{pv} , V_{pv} , I_{br} , V_{br} , I_{ev} , V_{ev}). All the inputs are compared with reference inputs and it generate pulses accordingly.

8 Sequence of switching operation

In Fig. 8, you can see a typical switching diagram. PV output is not available when the environment is cloudy. The power is transferred from ESS to EVCS via a bidirectional converter and a semi bridge converter in this case.

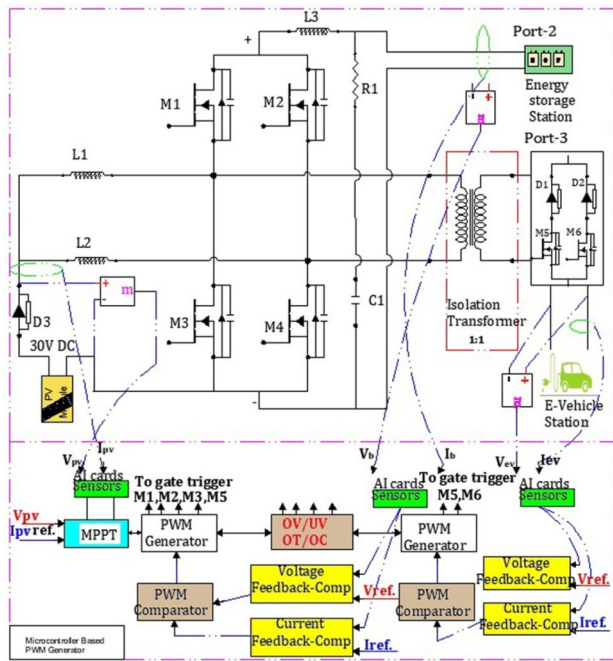


Fig. 7 Block diagram of PWM Controller

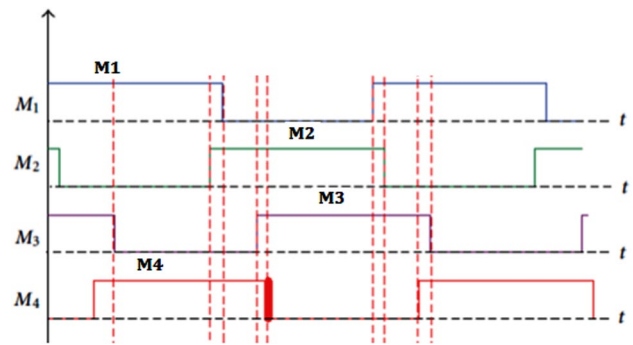


Fig. 9 Switching sequence pulse output wave form

9 Simulation and experimental results of the proposed system

Figure 10 depicts the suggested system's simulation circuit. The simulation of the suggested task is also carried out using MATLAB 2013 advanced version. PV module, MPPT, PWM generator, and power circuit make up the simulation circuit.

Through the isolation transformer, the power circuit consists of a bi-directional converter and a semi-bridge converter. The entire circuit is intended to handle 500 W of power, and all components were chosen accordingly. The numerical Mamdani model fuzzy rule results were tabulated in Table 2.

Figure 11 depicts the PV system's output voltage and current. The DC output voltage and DC output current of the three port converter are shown to be 31 V and 17 A, respectively. In addition, the X-axis indicates a time in seconds in which the DC input is continuous and the source is pure DC.

The output voltage and current of Port-2 fed to the ESS are shown in Fig. 12. It's also worth noting that the DC output voltage and current are 58 V and 7.8 A, respectively. The output voltage and current of Port-3 fed to the EVCS are shown in Fig. 13. The DC output voltage and DC output current are shown in Fig. 13 to be 13.8 V and 1.4 A, respectively.

Furthermore, the output voltage of port 3 is shown to be compatible with the voltage levels of E-vehicle batteries. The aforementioned simulated findings are adequate, thus the experiment can proceed. Figure 14 depicts the hardware setup of the proposed TPC. Further, the Bidirectional DC-DC boost converter unit, semi-bridge converter unit, Programmable Interface Controllers (PIC) microcontroller-based controller (disPIC30F2010), and accompanying driver circuits make up the hardware three port converter. The PIC controller also has six pulse outputs, each of which is fed into driver circuits. The optocoupler is

Fig. 8 Circuit diagram of switching sequence

Furthermore, the MOSFETs M1 and M4 conduct at time T1 and the positive cycle passes through the isolation transformer; during the conduction phase, the M2 conducts for smooth switching and the M1 provides commutation. Similarly, the switching pulse depicted in Fig. 9 shows M3 conducting and M4 providing commutation.

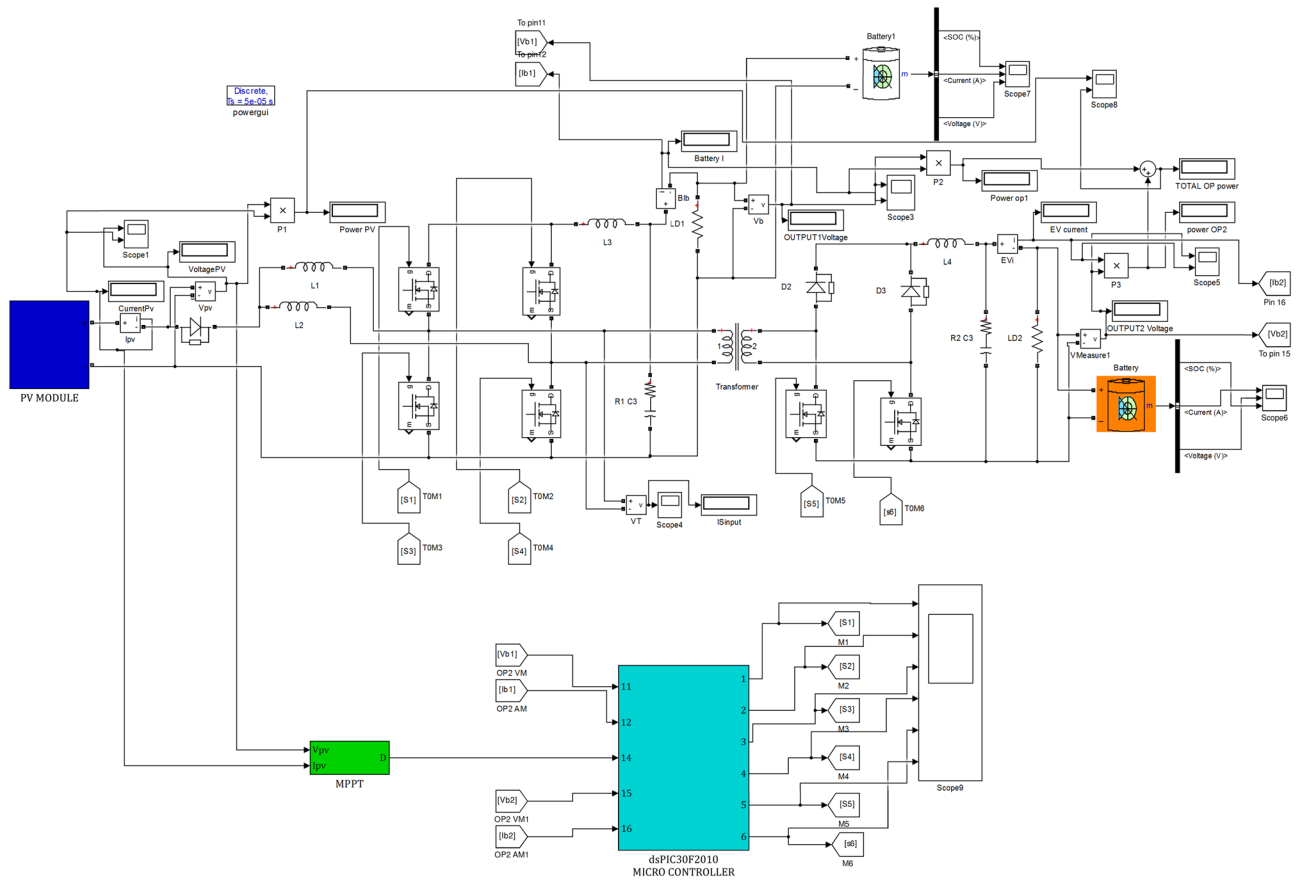


Fig. 10 Simulation diagram of proposed system

Table 2 Numerical tabulation for Mamdani model fuzzy rule

$\Delta(ek)\Delta(Pk)$	NB	NM	NS	ZE	PS	PM	PB
NB	5.5	5.5	5.3	5.3	5.1	5	5
NM	5.5	5.3	5.3	5.1	5	5	4.9
NS	5.3	5.3	5.1	5	5	4.9	4.9
ZE	5.3	5.1	5	5	4.9	4.9	4.7
PS	5.1	5	5	4.9	4.9	4.7	4.7
PM	5	5	4.9	4.9	4.7	4.7	4.5
PB	5	4.9	4.9	4.7	4.7	4.5	4.5

used to isolate the power and control circuits in the driving circuits.

The optocoupler output is connected to the gate signal of the MOSFET. Because the driver circuit and controller require a 5 V DC auxiliary power source, a separate transformer and rectifier circuit from an AC supply from the grid are used.

The bidirectional DC-DC boost converter absorbs input power from the PV module and provides output to the ESS and semi-bridge converter via an isolation transformer, where the zero volt switch is used and the primary side of the boost converter is involved in full Bridge topology

under the magnetization of the transformer taken as the function of inductance hints the duty cycle of DC-DC converter automatically adjusted for maximum power tracking [22]. Additionally, the Energy Storage Station has a 12 V battery bank for storing solar energy. In the event that solar energy is unavailable, the stored energy flows into the E-vehicle station.

The semi-bridge converter is a unidirectional DC-DC converter that supplies the e-Vehicle station with energy from solar energy and stored energy in the storage system via a bidirectional boost converter. Various types of DC-DC converters and their topologies that are utilised in PV

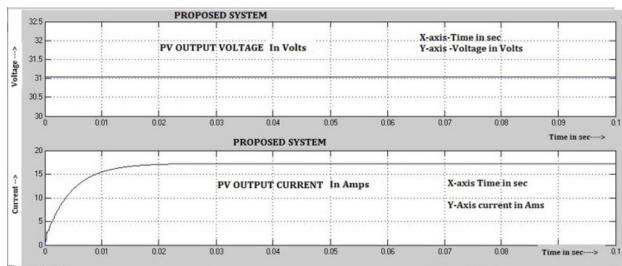


Fig. 11 PV output voltage and current waveform

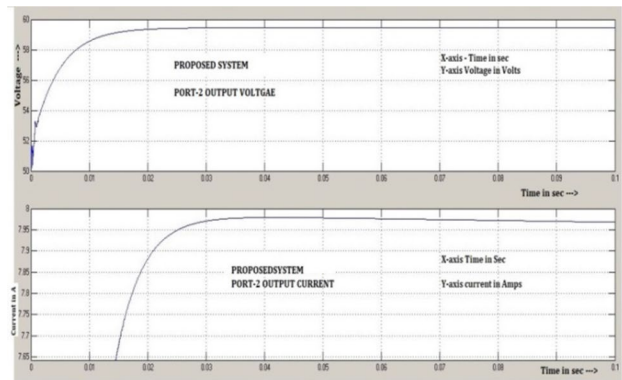


Fig. 12 Simulation results of port-2 output voltage and output current

applications are reviewed, and always impedance matching their favoured with a reduced number of switches is preferred [23].

Table 3 shows the technical specifications of the proposed three-port converter. In comparison to earlier literature, which had an efficiency of 91.3 percent [24], the proposed three-port converter is shown to have a 95.5 percent efficiency. The efficiency is boosted by introducing efficient switching techniques using a fuzzy controller, which results in less power loss by the switches. Our proposed three-port converter smoothes the output DC voltage and current using a restricted inductor and

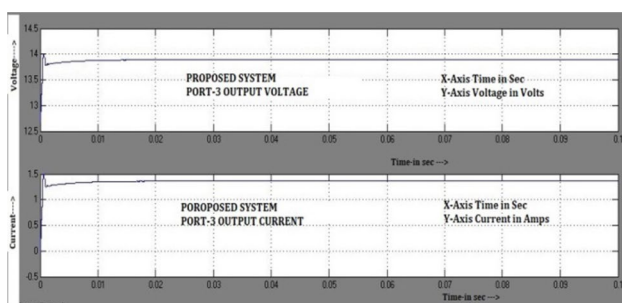


Fig. 13 Simulation results of port-3 output voltage and current

capacitor In a review publication, the efficiency of a three port converter with one transformer is 91.7% to 94%, but the efficiency of our suggested system is 95.5% [25]. The ESS and EVCS also have a 12 V rated output voltage.

The technical design parameters are listed in Table 4. The frequency used in this converter is 5 kHz, which was chosen based on the performance of the ripples that produce the least amount of noise.

The DC input current of the three-port converter is shown in Fig. 15. The input current is 1 amp, and the value is constant. By filtering the ripples, the input current wave is smooth.

As seen in Fig. 16, the output voltage of port 2 is 12 V. Smoothing with filtration technics raises the output voltage and fast achieves steady state, with no ripple. The output voltage of the twin converter is sent to the energy storage station. The smooth wave will always extend the battery's life.

Even when changing modes of operation and input current owing to solar changes, the output voltage remains highly smooth, whereas increasing efficiency results in non-smooth output voltage and current [26, 27].

The output voltage will be disturbed when the DC voltage in the converter is converted to AC voltage for domestic use, and when switching the domestic loads, the



Fig. 14 Developed hardware of the proposed system

Table 3 Technical specification of three port converter

Description	PV module	Energy storage station	E-vehicle station
Rated power	5W	2.4W	2.4W
Rated output voltage	5 V	12 V	12 V
Max output current	1A	200 mA	200 mA
Efficiency	95.5%		

Table 4 Technical parameter of three port converter

Description	Parameter
PV panel Power	5 W
Cell Voltage	5 V
Open circuit Voltage(Voc)	7.2 V
Open circuit Current(Ioc)	50 μ A
Short circuit Current	1.6 A
Temperature	± 45 $^{\circ}$ C
Irradiance	1000 W/cm ²
MOSFET	15 A
Frequency	5 kHz
Diode	10 A
Inductor	10 mH
Capacitor	100 μ F
Resistor	1 k Ω
Battery	12 V, 7 Ah, VRLA

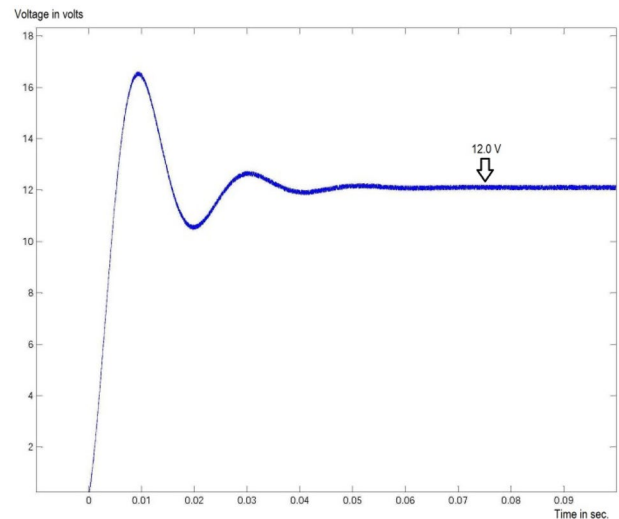


Fig. 16 Experimental results of port-2 output voltage

impact is on the battery discharge current, whereas our proposed system switches in such a way that it is stable and smooth under the same conditions [28].

In addition, the output voltage of port 3 is 12 V, as shown in Fig. 17. It is proved that the simulation and hardware output of proposed three port converter system is identical. Also, it is evident that the hardware output voltage of the proposed TPC is in line with voltage range of charging station. In port-3, the output voltage is raised and settled during initial changeover, whereas in port-2, the voltage is smoothly raised and settled due to the battery storage backup, whereas in the stand-alone situation, the voltage is smooth on lower ratings in both cases [29]. Further, it is observed that the proposed TPC is capable of holding output voltage in a stable manner.

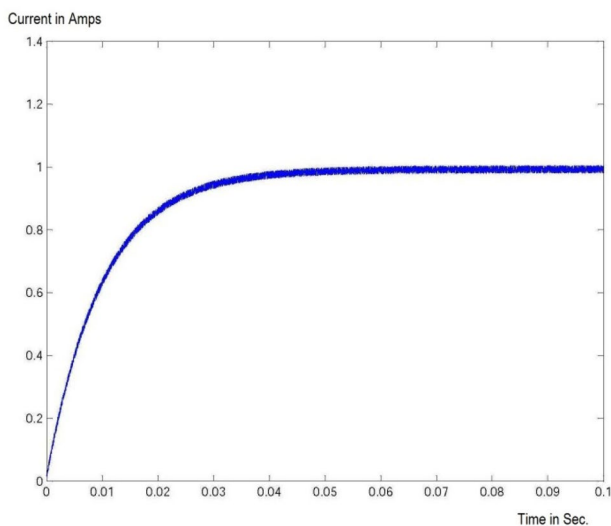


Fig. 15 DC Input current of the three-port converter

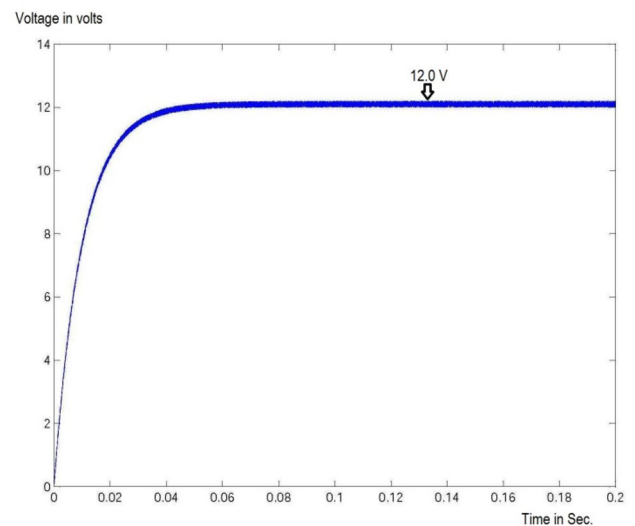


Fig. 17 Experimental results of port-3 output voltage

The proposed system has an efficiency of 95.5%, but a similar configuration on the modified full bridge three port converter has an efficiency of just 95%. As a result, when compared to total converters, our suggested system has the maximum efficiency, as demonstrated experimentally [30].

10 Conclusions

A simulation analysis was conducted for an existing TPC converter with a PWM controller, which revealed that the three independent DC-DC converters are required to obtain the output, requiring six MOSFETs per converter. As a result, the number of switches is increased, resulting in greater losses. Furthermore, the creation of a closed loop controller is quite challenging due to the poor feedback response. As a result of the sluggish switching and low response, a big capacitor is required to lower the ripple voltage on the output side.

In this work, a three-port converter with pulse width modulation and a phase shift controller was developed to alleviate the discussed disadvantages. The proposed system was also simulated, and portable hardware was developed. Furthermore, the proposed novel TPC utilizes lesser number of MOSFETs (6Nos.) and the proposed TPC's exhibit efficiency of 95.5 percent results in superior than existing converters. However, the general fuzzy MPPT has tuning difficulty of membership function and control rules, the MPPT and PWM with phase control method gains advantages such as smooth switching, rapid response, and low ripple at the output side. In addition, the proposed TPC uses a single common controller and a tiny capacitor to reduce output ripple, making the system highly portable. In near future, the advanced MPPT algorithms using evolutionary and Artificial Intelligence can be utilized and efficiency shall be increased.

Author contributions Primary and Corresponding author (KS) conceived, designed the model and drafted the paper. Co-author-1 (MN) created the simulink model and performed the simulation for the three port converter. Co-author-2 (AP) analyzes the simulation results and did the comparison with the conventional model. Co-author-3 (SV) has contributed in the experimental setup and provided us a very good academic support for establishing the experiment results.

Funding Not applicable.

Availability of data and materials The data sets generated during and/or analyzed during the current study are available from the corresponding author on reasonable request.

Declarations

Competing interest The authors declare no competing interests.

Open Access This article is licensed under a Creative Commons Attribution 4.0 International License, which permits use, sharing, adaptation, distribution and reproduction in any medium or format, as long as you give appropriate credit to the original author(s) and the source, provide a link to the Creative Commons licence, and indicate if changes were made. The images or other third party material in this article are included in the article's Creative Commons licence, unless indicated otherwise in a credit line to the material. If material is not included in the article's Creative Commons licence and your intended use is not permitted by statutory regulation or exceeds the permitted use, you will need to obtain permission directly from the copyright holder. To view a copy of this licence, visit <http://creativecommons.org/licenses/by/4.0/>.

References

1. de los Mozos AB, Mouli GRC, Bauer P (2019) Evaluation of topologies for a solar powered bidirectional electric vehicle charger. *IET Power Electron* 12(14):3675–3687. <https://doi.org/10.1049/iet-pel.2018.5165>
2. Gan C, Jin N, Sun Q, Kong W, Hu Y, Tolbert LM (2018) Multiport bidirectional SRM drives for solar-assisted hybrid electric bus power train with flexible driving and self-charging functions. *IEEE Trans Power Electron* 33(10):8231–8245. <https://doi.org/10.1109/TPEL.2017.2780622>
3. AC Nair, BG Fernandes (2018) A solid-state transformer based fast charging station for all categories of electric vehicles. In: *IECON 2018—44th annual conference of the IEEE industrial electronics society*, Washington, DC, USA, pp 1989–1994. <https://doi.org/10.1109/IECON.2018.8592739>
4. Chandra Mouli GR, Bauer P, Zeman M (2016) System design for a solar powered electric vehicle charging station for workplaces. *Appl Energy* 168:434–443. <https://doi.org/10.1016/j.apenergy.2016.01.110>
5. Denholm P, Kuss M, Margolis RM (2013) Co-benefits of large scale plug-in hybrid electric vehicle and solar PV deployment. *J Power Sources* 236:350–356. <https://doi.org/10.1016/j.jpowsour.2012.10.007>
6. Taghizadeh S, Hossain MJ, Poursafar N, Lu J, Konstantinou G (2020) A Multifunctional single-phase EV on-board charger with a new V2V charging assistance capability. *IEEE Access* 8:116812–116823. <https://doi.org/10.1109/ACCESS.2020.3004931>
7. Nagarjun S, Debnath D, Chakraborty C (2020) Synthesis of three-port converter from existing dc-dc converters for PV based dc stand-alone system. In: *IEEE international conference on power electronics, smart grid and renewable energy (PESGRE2020)*, Cochin, India, pp 1–6. <https://doi.org/10.1109/PESGRE45664.2020.9070443>
8. Iyer VM, Gulur S, Gohil G, Bhattacharya S (2018) Extreme fast charging station architecture for electric vehicles with partial power processing. In: *IEEE applied power electronics conference and exposition (APEC)*, San Antonio, TX, USA, pp 659–665. <https://doi.org/10.1109/APEC.2018.8341082>
9. Wu J, Liu B, Wu X, Qi H (2018) Research on a new three-port converter operating principle and control strategy. *Energy Procedia* 152:204–209. <https://doi.org/10.1016/j.egypro.2018.09.081>
10. Zhu H, Zhang D, Athab HS, Wu B, Gu Y (2015) PV isolated three-port converter and energy-balancing control method for

- PV-battery power supply applications. *IEEE Trans Ind Electron* 62(6):3595–3606. <https://doi.org/10.1109/TIE.2014.2378752>
11. Hu Y, Xiao W, Cao W, Ji B, Morrow DJ (2015) Three-port DC–DC converter for stand-alone photovoltaic systems. *IEEE Trans Power Electron* 30(6):3068–3076. <https://doi.org/10.1109/TPEL.2014.2331343>
 12. Prem P, Sivaraman P, Sakthi Suriya Raj JS, Jagabar Sathik M, Almakhlles D (2020) Fast charging converter and control algorithm for solar PV battery and electrical grid integrated electric vehicle charging station. *Automatika* 61(4):614–625. <https://doi.org/10.1080/00051144.2020.1810506>
 13. Khan W, Ahmad F, Alam MS (2019) Fast EV charging station integration with grid ensuring optimal and quality power exchange. *Eng Sci Technol Int J* 22(1):143–152. <https://doi.org/10.1016/j.jestch.2018.08.005>
 14. Mouli GRC, Bauer P, Zeman M (2015) Comparison of system architecture and converter topology for a solar powered electric vehicle charging station. In: 2015 9th international conference on power electronics and ECCE Asia (ICPE-ECCE Asia), Seoul, Korea (South), pp 1908–1915. <https://doi.org/10.1109/ICPE.2015.7168039>
 15. Ning G et al (2017) Hybrid resonant VZCS PWM full-bridge converter for large photovoltaic parks connecting to MVDC grids. *IEEE J Emerg Sel Top Power Electron* 5(3):1078–1090. <https://doi.org/10.1109/JESTPE.2017.2651020>
 16. Zeng J, Qiao W, Qu L (2013) An isolated three-port bidirectional DC-DC converter for photovoltaic systems with energy storage. In: 2013 IEEE industry applications society annual meeting, Lake Buena Vista, FL, USA, pp 1–8. <https://doi.org/10.1109/IAS.2013.6682520>
 17. Moradisizkoohi H, Elsayad N, Shojaie M, Mohammed OA (2019) PWM plus phase-shift-modulated three-port three-level soft-switching converter using GaN switches for photovoltaic applications. *IEEE J Emerg Sel Top Power Electron* 7(2):636–652. <https://doi.org/10.1109/JESTPE.2019.2904243>
 18. Tu H, Feng H, Srdic S, Lukic S (2019) Extreme fast charging of electric vehicles: a technology overview. *IEEE Trans Transp Electr* 5(4):861–878. <https://doi.org/10.1109/TTE.2019.2958709>
 19. KiranKumar KV, Noorshiba P, Jyothi B, Srikanth M (2020) Fast charging of Ev by reducing grid side harmonics in the rectifier using five phase supply. *J Crit Rev* 7(9):308–312
 20. da Câmara RA, Fernández-Ramírez LM, Praça PP, Oliveira DS, García-Triviño P, Sarrias-Mena R (2019) An application of the multi-port bidirectional three-phase AC-DC converter in electric vehicle charging station microgrid. In: IEEE 15th Brazilian power electronics conference and 5th IEEE southern power electronics conference (COBEP/SPEC), Santos, Brazil, pp 1–6. <https://doi.org/10.1109/COBEP/SPEC44138.2019.9065752>
 21. Kumar V, Teja VR, Singh M, Mishra S (2019) PV based off-grid charging station for electric vehicle. *IFAC-papers on line* 52(4):276–281. <https://doi.org/10.1016/j.ifacol.2019.08.211>
 22. Hu W, Wu H, Xing Y, Sun K (2014) A full-bridge three-port converter for renewable energy application. In: 2014 IEEE applied power electronics conference and exposition—APEC 2014, Fort Worth, TX, USA, pp 57–62. <https://doi.org/10.1109/APEC.2014.6803289>
 23. Xu P, Wen H (2020) Topology review of three-port DC-DC converters for photovoltaic applications. In: 2020 IEEE/IAS industrial and commercial power system Asia (I&CPS Asia), Weihai, China, pp 1216–1221. <https://doi.org/10.1109/ICPSAsia48933.2020.9208398>
 24. Lu Y, Wu H, Dong X, Xing Y, Sun K (2017) A three-port converter-based DC grid-connected PV system with autonomous output voltage sharing control. In: IEEE applied power electronics conference and exposition (APEC), Tampa, FL, USA, pp 2057–2061. <https://doi.org/10.1109/APEC.2017.7930982>
 25. Zhang N, Sutanto D, Muttaqi KM (2016) A review of topologies of three-port DC-DC converters for the integration of renewable energy and energy storage system. *Renew Sustain Energy Rev* 56:388–401
 26. Boppearachchi L, Liyanage HS, Dasanayake VH, Chandima DP, Bolonne S (2021) Efficiency enhanced three-port DC-DC converter for MPPT controlled solar-battery systems. In: 2021 3rd international conference on electrical engineering (EECon), Colombo, Sri Lanka, pp 100–105. <https://doi.org/10.1109/EECon52960.2021.9580865>
 27. Liang T-J, Tran TAA, Huynh KKN, Chen K-H, Chen S-M (2023) High step-up three-port converter for renewable energy systems. *IEEE Access* 11:47432–47447. <https://doi.org/10.1109/ACCESS.2023.3275731>
 28. Lee H-S, Yun JJ (2020) Three-port converter for integrating energy storage and wireless power transfer systems in future residential applications. *Energies* 13(1):272. <https://doi.org/10.3390/en13010272>
 29. Selvabharathi D, Vishwas P, Saurav P, Babu S, Selvakumar K (2020) Design of stand alone photovoltaic system using three port Dc-Dc converter. *Int J Electr Eng Technol IJEET* 11(3):155–163
 30. Zhu L, Wu H, Xu P, Hu H, Ge H (2014) A novel high efficiency high power density three-port converter based on interleaved half-bridge converter for renewable energy applications. In: 2014 IEEE energy conversion congress and exposition (ECCE), Pittsburgh, PA, USA, pp 5085–5091. <https://doi.org/10.1109/ECCE.2014.6954099>

Publisher's Note Springer Nature remains neutral with regard to jurisdictional claims in published maps and institutional affiliations.